LASER BASED SUB-PICOSECOND ELECTRON BUNCH CHARACTERIZATION USING 90˚ THOMSON SCATTERING*

W. P. Leemans, P. Volfbeyn, M. Zolotorev, K-J. Kim, S. Chattopadhyay, R. W. Schoenlein, A.H. Chin, T.E. Glover, P. Balling, and C. V. Shank, LBL, Berkeley, CA 94720 USA

X-rays produced by 90˚ Thomson scattering of a femtosecond, near infrared, terawatt laser pulse off a 50 MeV electron beam are shown to be an effective diagnostic to measure transverse and longitudinal density distributions of an electron beam (e-beam) with subpicosecond time resolution. The laser beam was focused onto the e-beam waist, generating 30 keV x-rays in the forward direction. The transverse and longitudinal e-beam structure have been obtained by measuring the intensity of the x-ray beam, while scanning the laser beam across the e-beam in space and time. The e-beam divergence has been obtained through measurement of spatial and spectral characteristics of the scattered x-ray beam.

1 INTRODUCTION

Measurement of the transverse and longitudinal phase space properties of electron bunches produced with high performance linear accelerators, requires development of beam diagnostics with high spatial (micron or sub-micron) and temporal (femtosecond) resolution requirements. A laser based beam diagnostic [1] has been developed and used at the Beam Test Facility (BTF) [2] of the Center for Beam Physics at Lawrence Berkeley National Laboratory (LBNL).

2 EXPERIMENT

A. Electron Transport Line and Laser Beam Parameters

The experiment[1,3] was conducted at the BTF and used the linear accelerator (linac) injector of the Advanced Light Source in conjunction with a terawatt short pulse laser system. The lay-out of the experiment is shown in Fig. 1.

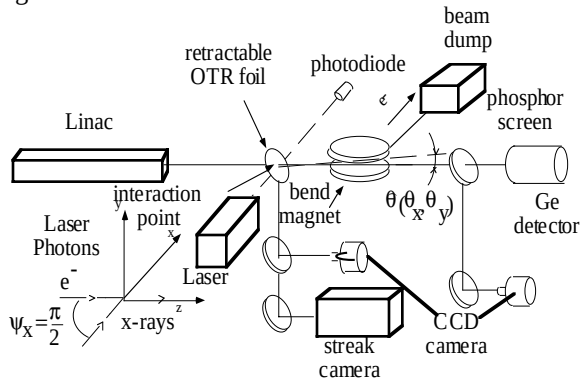

Figure 1: Lay-out of the laser probe experiment.

Electron bunches were transported using bend magnets and quadrupoles to an interaction chamber where they were focused and scattered against the laser beam. After the interaction chamber, a 60˚ bend magnet deflected the electron beam onto a beam dump, away from the forward scattered x-rays. The measured electron beam parameters are given in Table 1.

Maximum Energy	50 MeV
Charge	1.3 -1 .5 nC/bunch
Bunch Length (σ_z)	10-15 ps
Emittance rms (unnorm)	0.3 mm-mrad
# bunches/macropulse @ 125 MHz	1 - 10 (max 100)
Macropulse rep. rate	1 - 5 Hz

Table 1: ALS Linac parameters

The terawatt laser system, with center wavelength at 800 nm, was based on chirped pulse amplification in Ti:Al_2O_3 [4]. The laser system parameters are shown in Table 2. A 75 cm radius of curvature mirror was used to focus the S-polarized amplified laser pulses to about a 30 μm diameter spot at the IP (measured by a charge coupled device (CCD) camera at an equivalent image plane outside the vacuum chamber).

Wavelength	0.8 μm
Energy/pulse	50 mJ
Pulse length	50 - 200 fs
Repetition rate	10 Hz
Timing jitter with e-beam	< 2 ps

Table 2: Laser system parameters

To measure the spot size (and position) of the electron beam at the interaction point (IP), an image of the electron beam was obtained by relaying optical transition radiation (OTR) [5] from a foil onto a 16 bit CCD camera or optical streak camera using a small f-number telescope. Electron beam spot sizes as small as 35 μm rms have been measured.

Synchronization between the laser oscillator and linac was accomplished by using a phase-locked loop which dynamically adjusts the oscillator cavity length [6]. Timing jitter measurements (using a streak camera with an instrument response of 1.5 - 2 ps) which simultaneously detected a laser pulse and OTR from the electron bunch indicated an rms jitter of 1-2 ps.

During the interaction of an electron beam and laser beam, scattered x-ray photons are produced with energy U_x, given by (for $\gamma >> 1$)

$$U_x = \frac{2\gamma^2\hbar\omega_0}{1+\gamma^2\theta^2}(1-\cos\psi) \qquad (1),$$

where ω_0 is the frequency of the incident photons, ψ is the interaction angle between the electron and laser beam ($\psi=\pi/2$ in our experiments) , and θ is the angle at which the radiation is observed and assumed to satisfy $\theta << 1$ (see Fig. 1). When the 50 MeV electron beam (γ = 98) collides at 90˚ with the laser pulse (center wavelength =

* This work was supported by DOE under contract No. DE-AC03-76SF00098.

800 nm), x-rays with a maximum energy of 30 keV (0.4 Å) are generated. The x-ray beam parameters are shown in Table 3.

Wavelength (Å)	0.4
Pulse length (fs)	200
# photons (10 % bandwidth)	1 x 10^5
Full angle cone (mrad)	10
Bandwidth (%)	10-15%

Table 3: x-ray source parameters.

B. Electron beam characterization

To measure the transverse electron beam distribution for a given slice of the electron beam, we scanned the laser beam transversely across the electron beam in steps of 10 μm, by changing the tilt of the focusing mirror. and monitored the x-ray yield on the phosphor screen. It was found (Fig. 2) that the laser based technique and the results from OTR were in good agreement and give a half-width half maximum (HWHM) vertical size of 66 μm. However, whereas the beam core overlaps, the tails are different and both non-Gaussian. From the OTR data an HWHM horizontal size of 47 μm was obtained.

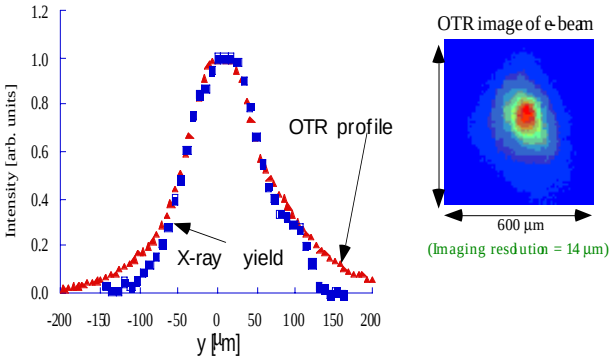

Figure 2: a) OTR image of the focused electron beam and b) s (triangle) - vertical line-profile through the OTR image of the electron beam; ¸ (square)- x-ray yield vs. vertical laser beam position.

Measurement of the electron beam divergence for a fixed longitudinal location (i.e. fixed delay time between the laser and electron beam) of a time slice of the electron beam, with a duration equal to the convolution of the transit time of the laser pulse and the laser pulse duration, was done by monitoring the spatial x-ray beam profile on the phosphor screen using the CCD camera (see Fig.(3)). The scattered x-ray energy flux contains information of the angular distribution of the electron beam. By convoluting the single electron spectrum [7] with a Gaussian distribution for the horizontal and vertical angles ($\sigma_{\theta x}$ and $\sigma_{\theta y}$ are the rms. widths of the angular distribution of the electron beam in the horizontal and vertical direction respectively) and integrating over all energies and solid angle[1] the energy flux can be written as:

$$\frac{dP}{d\theta_x d\theta_y} \propto \int_0^{2\pi} d\phi \int_0^1 d\kappa F(\kappa)\kappa\left[1-4\kappa(1-\kappa)\cos^2\phi\right] \exp\left[-\frac{(\theta_x-\gamma^{-1}\sqrt{\frac{1}{\kappa}-1}\cos\phi)^2}{2\sigma_{\theta x}^2}\right] \exp\left[-\frac{(\theta_y+\gamma^{-1}\sqrt{\frac{1}{\kappa}-1}\sin\phi)^2}{2\sigma_{\theta y}^2}\right] \quad (2).$$

Here dP is the radiated x-rays intensity in a solid angle $d\theta_x d\theta_y$, ϕ is the azimuthal angle and F(κ) is an x-ray energy dependent function which takes into account overall detector sensitivity and x-ray vacuum window transmission, $\kappa = U/U_{\max} = (1+\gamma^2\theta^2)^{-1}$ with $U_{\max} = 2\gamma^2\hbar\omega$ and we have assumed a single incident laser frequency.

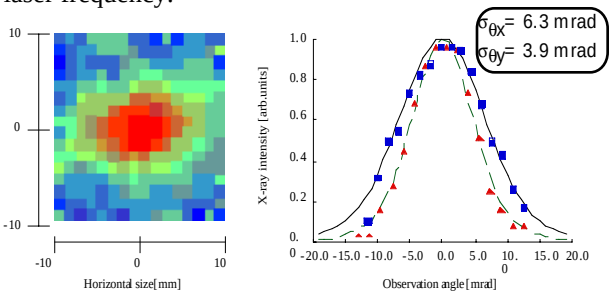

Figure 3. a) False color CCD image of the spatial profile of a 30 keV x-ray pulse on the phosphor screen, which is located 80 cm from the IP; b) ¸ (square)- horizontal line-profile and fitting curve (solid line), s (triangle) -vertical line-profile and fitting curve (dashed line) from Fig. 3 (a). The scale has been converted into angular units.

By fitting the data (see Fig. 3) using Eq.(2), an electron beam divergence of $\sigma_{\theta x}$ ($\sigma_{\theta y}$) = 6.3 ± 0.2 (3.9 ± 0.2) mrad was found. F(κ) was adjusted to account for the spectral dependence of the x-ray window transmission. The difference between $\sigma_{\theta x}$ and $\sigma_{\theta y}$, is due to a combination of, the electron beam being focused astigmatically at the IP, resulting in a tilted phase space ellipse (y, y′), and a laser spot size much smaller than the vertical electron beam size. As the laser beam crosses the focal volume of the electron beam, the complete horizontal (direction of propagation of the laser) phase space (x, x′) is sampled by the laser beam. However, only electrons occupying the region in the vertical phase space defined by the spatial overlap with the laser beam will contribute to the x-ray flux. As opposed to the transition radiation based detector, the laser beam therefore acts as an optical microprobe of a finite region of the transverse phase space. This value of the electron beam divergence is also consistent with an effective angular divergence of the electron beam of 3.5 - 4 mrad obtained from analyzing the x-ray spectra. Of course, the main difference is that measurement of the spatial profile is a single shot technique as opposed to measuring the x-ray spectra which requires accumulation of thousands of shots.

The spot size measurements and beam divergence measurements imply a horizontal geometric slice emittance $\sigma_x \sigma_{\theta x}$ for the electron beam of 0.25±0.03 mm-mrad. A linac beam emittance of 0.32±0.02 mm-mrad was measured using a quadrupole scan technique [8], which is in reasonable agreement with the x-ray slice measurements.

Finally, since the x-ray yield is sensitive to both the longitudinal bunch profile and the degree of transverse overlap between the laser and electron beam, time-correlated phase space properties of the electron beam can be studied. When an electron bunch, which exhibits a finite time-correlated energy spread (chirp), is focused at the IP with a magnetic lattice which has large chromatic aberrations, different temporal slices of the bunch will be focused at different longitudinal locations. The transverse overlap between e-beam and laser will therefore strongly depend on which time slice the laser interacts with. This in turn will lead to a time dependence of the x-ray yield varying faster than the actual longitudinal charge distribution. To illustrate this, the x-ray flux was measured as a function of the delay between laser and e-beam, for two different magnetic transport lattices. In both lattices, the magnet settings were optimized to obtain a minimum electron beam spot size in the horizontal and vertical plane (as well as zero dispersion at the IP), but chromatic aberrations were about 5 times larger in the second lattice. Result of a 60 ps long scan (time step of 1 ps) and time-resolved OTR from the streak camera for the lattice with low and high chromatic aberrations is shown in Fig. 4(a, b).

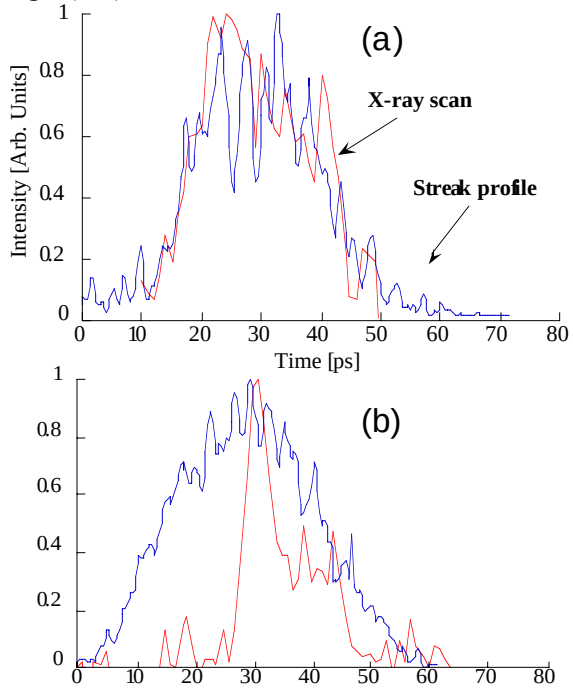

Figure 4: x-ray yield vs. delay time between laser and electron beam and profile of time resolved OTR image from a streak camera for a lattice with a) small and b) large chromatic aberrations.

Whereas the temporal scan for the lattice with low chromatic aberrations (Fig.4a) is in good agreement with the time-resolved OTR measured with a visible streak camera, the scans taken for the second configuration (Fig.4b) typically showed a 2-3 times larger amplitude 5 ps wide peak sitting on a 20 ps wide pedestal. This is to be compared to the time resolved OTR from the streak camera which typically showed a 25-30 ps wide electron beam without any sharp time structure. Lattice calculations for our experiment with MAD [9] indicated that an energy change of 0.25 % would increase the vertical spot size by a factor two at the IP, compared to best focus, resulting in a proportional reduction in vertical overlap between the laser and electron beam, and hence in x-ray yield. The measurements indicate the potential of the laser based Thomson diagnostic to measure time-correlated energy changes of less than a percent, with sub-picosecond time resolution.

3 SUMMARY

Laser based probing of electron beams has been used for measurement of longitudinal and transverse bunch distributions of picosecond and sub-picosecond slices. From a study of x-ray beam images and total flux, the transverse electron beam phase space distribution of essentially a 300 fs slice of the electron beam was obtained. By scanning the laser beam in time along the electron bunch, not only the longitudinal density distribution was measured, but it was also found that the Thomson scattering technique can become a powerful and sensitive tool to measure detailed longitudinal phase space properties. The main limitation on the slice duration arose from the finite transit time of the laser pulse across the electron beam. Shorter slices and higher photon yields are expected when using RF photocathode guns which produce beams with normalized emittance on the order of a few π mm-mrad. Synchronization jitter between the laser and the linac were experimentally found to be on the order of a picosecond. The laser based method is best suited for photocathode driven RF guns, where lower jitter between laser and electron beam is expected.

4 ACKNOWLEDGEMENTS

The authors wish to thank the ALS personnel for their help in the operation of the BTF, in particular Terry Byrne. We would also like to thank Leon Archambault and Jim Dougherty for engineering and technical support.

5 REFERENCES

[1] W.P. Leemans et al., Phys. Rev. Lett.**77**, pp. 4182 (1996).
[2] W. P. Leemans et al., Proc. 1993 Part. Accel. Conf, 83 (1993).
[3] R.W. Schoenlein et al., Science **274**, pp.236-238(1996)
[4] D. Strickland and G. Mourou, Opt. Comm. **56**, 219 (1985); C. LeBlanc, et al., Opt. Lett. **18**, 140 (1993).
[5]L. Wartski, J. Marcou and S. Roland, IEEE Trans. in Nucl. Science, vol. 20, pp. 544 (1973).
[6]M.J.W. Rodwell, D.M. bloom, K.J. Weingarten, IEEE J. Quant. Electron. **25**, 817 (1989).
[7] K.- J. Kim, S. Chattopadhyay and C.V. Shank., NIMA 341, 351 (1994).
[8] J. Bengtson, W. Leemans, and T. Byrne, Proc. 1993 Particle Accelerator Conf., pp. 567(1993).
[9] H. Groter and F. Iselin, "The MAD program", CERN/SL/90-13 (1993).